C.P. No. 965

C.P. No. 965

MINISTRY OF TECHNOLOGY

AERONAUTICAL RESEARCH COUNCIL

CURRENT PAPERS

Heat Transfer in the Vicinity of a 15° Compression Corner at Mach Numbers from 2.5 to 4.4

by

, C. S. Brown and Susan Atkinson

ER MAJESTY'S STATIONERY OFFICE

1967

CE SEVEN SHILLINGS NET

U.D.C. No. 533.6.011.6 : 536.55 : 533.6.011.5 : 532.552

C.P. No. 965*
June 1966

HEAT TRANSFER IN THE VICINITY OF A 15° COMPRESSION CORNER AT MACH NUMBERS FROM 2.5 TO 4.4

by

R. C. Hastings
C. S. Brown
Susan Atkinson

SUMMARY

Commercially available heatmeters have been used to measure the steady-state heat transfer rates in the vicinity of a compression corner. Results at all Mach numbers are qualitatively similar in that, both ahead and downstream of the corner, the measured heat transfer rate was lower than expected.

In the compression region close to the corner, the adiabatic wall temperatures were also low.

The measuring technique is discussed and some potential sources of error are indicated.

---

* Replaces R.A.E. Technical Report No. 66171 - A.R.C. 28406.

CONTENTS

1 INTRODUCTION

Heat transfer rates have been measured in the neighbourhood of a 15° compression corner. The Mach number of the flow approaching the corner was varied from 2.5 to 4.36, corresponding to a Reynolds number range of 13.25 to 8.33×10^6 per foot.

The tests were undertaken with applications such as multi-shock intakes in mind. The corner angle was chosen so that it would generate a shock wave which, while fairly strong, would not separate a turbulent boundary layer.

Heat transfer rates were measured by the steady state technique developed by Naysmith[1]. The present state of this method is discussed in detail since it bears on the conduct of the tests and the validity of the results presented here.

2 TECHNIQUE FOR MEASURING STEADY HEAT FLOW

The basis of the method is that sensitive heatmeters, commercially available, are embedded, together with surface-temperature thermocouples, in the skin of an internally cooled model. Rate of heat flow into the skin and skin surface temperature can then be related. The arrangement is shown in Fig.3(a) and 3(b) is a diagram of a heatmeter disc.

The heatmeter discs, developed by Hatfield[2], give an electrical signal when subjected to heat flow in a direction which produces a temperature difference between their opposite faces. The signal is generated thermo-electrically at the junctions between copper electrodes and the faces of the tellurium-silver disc. The high sensitivity of these meters compared for example with a meter consisting of a constantan disc with copper electrodes, is due to two factors, namely a tenfold increase in thermo-electric power and a decrease of the same order in thermal conductivity. The manufacturer supplies a calibration factor with each heatmeter, giving the voltage output for unit heat flow normal to the faces of the disc. This calibration relates to fairly small heat flows, about 0.1 CHU per sq ft per second, at a temperature of about 15°C. Arising from the tests reported here, there are some doubts about the applicability of these calibrations to heatmeters mounted in cold models.

The thermal conductivity and thermo-electric power of a sample of tellurium-silver alloy, about 3 inches diameter by $\frac{1}{4}$ inch thick, were measured in the Basic Physics Division of the National Physical Laboratory under the supervision of Dr. R.W. Powell whose assistance is gratefully acknowledged. The conductivity was found to be 1.9×10^{-4} CHU per ft second °C at 30°C and

2.3×10^{-4} CHU per ft second $^{\circ}$C at -60°C. The thermo-electric emf generated at a junction between the sample and a copper wire changed at a rate of 450 μV per $^{\circ}$C in the range -190°C to 40°C. This sample was of course much larger than the ordinary heatmeter disc (the size was dictated by the method of measuring the conductivity) and the material was found to be harder and more brittle than that used in the heatmeters. It is not known what effect these differences may have had on the thermal and electrical behaviour.

In order that heatmeters can correctly measure heat flow to the surface of a model, the model skin should have a thermal conductivity close to that of the meters. This condition has been achieved by embedding the meters in a surface coating of epoxy resin, loaded with about 1.2 times its own weight of fine aluminium particles. The low conductivity of this coating has the advantage that it reduces conductivity along the skin, so enabling sharp peaks in heat flow (e.g. near re-attachment in rearward-facing step flows[1]) to be measured. This same property however limits heat flow into the model for a given internal coolant temperature and it is thus desirable to keep skin thickness to a minimum. The limit on skin thickness together with the need to study non-uniform distributions of heat flow lead to a requirement for small, thin heatmeters. Such meters are currently being developed and improved methods of calibration are being sought*, which in future should cover wider ranges of heat flow and temperature. It is hoped to make calibration easier and quicker by reducing the thermal inertia inherent in calibrators based on Hatfield's original design[2].

3 EXPERIMENTAL APPARATUS

3.1 Model

Fig.1 shows the general arrangement of the model with leading dimensions, while Fig.2 shows in cross-section the internal construction.

A gunmetal casting provides a manifold for the coolant, together with inlet and outlet passages. A perforated brass plate covers the manifold and forms the bottom of the coolant chamber. The top of the coolant chamber is another brass plate, which, on its outer surface, carries the resin skin, and the instrumentation.

Static pressure tubes were sweated to the brass plate, while heatmeters were attached to it by a thin film of resin. With these components in place the resin skin was first cast on, then worked to give a smooth, flat surface.

Thermocouples were installed as shown in Fig.3(a), and finally 0.020 inch diameter pressure holes were drilled through the skin into the hypodermic tubes.

* See footnote to p. 14.

Pressure tubes and electrical leads were all taken out spanwise without crossing the chordwise centre-line in order to minimise interference with heat transfer near this line. The positions of the pressure orifices, heatmeters and thermocouples are listed in Table 1.

The span of the model was large enough to ensure that the region (at least outside the boundary layer) influenced by the tips remained several inches clear of the chordwise centre-line. This is indicated in Fig.1.

3.2 Model cooling equipment

The circuit diagram of the equipment used for cooling the model is shown in Fig.4. The equipment is only slightly different from that used by Naysmith and described by him in Ref.5. Non-inflammable trichloroethylene is now used in place of alcohol as the heat transport medium, necessitating the replacement of all rubber parts such as seals, flexible hoses etc, by similar parts made from nylon.

The temperature of the circulating fluid and therefore the model, is controlled by selecting the proportion of the total flow allowed to pass through the cooler. The cooler itself is simply a coil of copper tube immersed in a tank containing a mixture of solid carbon dioxide and trichloroethylene.

3.3 Wind tunnel

The tests were made in the High Supersonic Speed Wind Tunnel at R.A.E. Bedford. This is a closed circuit, continuous flow tunnel with a working section 4 ft by 3 ft. At the time of the tests a wooden nozzle provided a fixed Mach number nominally equal to 4. Stagnation pressure can be varied between 15 and 220 inHg.

This facility has been described in detail in Refs.3 and 4.

3.4 Data recording facilities

Pressure tubes were led to the Midwood[6] self-balancing capsule manometers, which are standard ancillaries to the tunnel. These instruments measure absolute pressures up to 60 inHg, with an accuracy of ±0.02 inHg on digitised output.

Thermocouple and heatmeter voltages were measured by the self-balancing d.c. potentiometers normally used in conjunction with strain-gauge force balances. For heat transfer tests each potentiometer has been fitted with a twelve-way switch which is scanned automatically. The twelve positions are covered in about 20 seconds. With ten potentiometers available for simultaneous scanning, this is the total time required to record from any number up to 60 measuring stations. (Each station requires a channel for a thermocouple and another for a heatmeter.) Ranges of 1, 2, 4 ...... 32 millivolts are available, with an accuracy better than $\frac{1}{2}$% of full-scale.

Information from digitisers, fitted to the manometers and potentiometers, is punched on to cards which constitute both the data record and the input to an automatic computer.

4 DESCRIPTION OF TESTS

Because the free stream Mach number in the high-supersonic wind tunnel was at the time of these tests fixed at $M = 4$, a range of different Mach numbers upstream of the corner was obtained by pitching the model. At each Mach number the model temperature was changed in a series of steps and at each constant temperature heat flow and temperature were recorded.

At the beginning of the tests, before an operating technique for the cooling plant had been established, some difficulty was experienced in maintaining constant temperatures. This is reflected in the scatter of data at the lowest Mach number, which was the first of the series. To gauge the importance of temperature variation, some data were obtained later with continuously varying temperature.

Because of the possibility of failure of the model skin, cooling was limited in the first test to about 10°C below recovery temperature. In subsequent tests the model was cooled progressively further, finally reaching about 30°C below recovery (i.e. about -10°C).

The maximum rate of heat transfer did not, however, change very much from one test to another, and was of the order of 0.1 CHU per square foot per second.

Test conditions are summarised in Table 2, which also gives the approximate total pressures above which no boundary layer separation on the model was visible on the schlieren screen.

All data were obtained at a total pressure of 220 inHg and a total temperature of 40°C as measured in the tunnel settling chamber.

The specific humidity of the airstream was between 140 and 200 parts per million by weight. The reference junctions of the thermocouples were maintained at 50°C in a temperature controlled water bath.

5 DATA REDUCTION AND THEORY

In reducing the heat flow and temperature results, advantage has been taken of the capacity of automatic computing in order to remove some sources of error. The computer programme allows non-linear calibrations for both thermocouples and heatmeters to be used and ensures that both heat flow and temperature at each data point, are non-dimensionalised with the aid of total pressure and temperature measured at the same time.

At this stage of the process, the data are available as:-

$$\pi = \frac{Q}{(\rho u C_p T)_a} \text{, a non-dimensional heat flow}$$

$$\tau = \frac{T_w}{(T)_a} \text{, a non-dimensional temperature}$$

where Q = heat transfer rate per unit area
ρ = air density
u = air velocity
T = air static temperature
T_w = model surface temperature
C_p = specific heat of air at constant pressure

and suffix a denotes a reference flow condition used in forming non-dimensional variables.

The reference condition, which must be constant, is computed automatically from free stream total pressure and total temperature, if reference Mach number and the ratio of free stream total pressure to total pressure at the reference state, are supplied to the computer. The data, in this form, can be plotted mechanically as graphs of π versus τ for each measuring station.

The final results are obtained from a straight line, fitted by the "least-squares" method, to the π and τ data. Firstly the slope of the line, and the value of τ at $\pi = 0$; i.e. zero heat transfer, are found. From these, Stanton number and recovery factor corresponding to the reference Mach number M_a, are computed.

By definition:-

$$Q = \rho u C_p S_T (T_r - T_w) \quad ,$$

if T_r = recovery temperature (temperature at zero heat transfer)

and S_T = Stanton number .

Hence, if Q is linearly related to T_w,

$$\frac{dQ}{dT_w} = -\rho u C_p S_T ,$$

so that

$$\frac{d\pi}{d\tau} = -(S_T)_a ,$$

if

$$(S_T)_a = \frac{Q}{(\rho u C_p)_a (T_r - T_w)} .$$

The recovery factor, r, is defined by:-

$$\frac{(T_w)_{Q=0}}{T} = 1 + \left(\frac{\gamma - 1}{2}\right) r M^2 ,$$

so that

$$(r)_a = [(\tau)_{\pi=0} - 1] \frac{2}{(\gamma - 1) M_a^2} .$$

The computer output consists of $(S_T)_a$ and $(r)_a$ for each measuring station along the model, together with values of $(T)_a$ and "unit" Reynolds number $\left(\frac{\rho u}{\mu}\right)_a$ averaged over all the data points making up a complete run.

Figs.5 and 6 show the linearity of the heat flow versus temperature relations measured in the tests. The examples have been chosen to cover the whole test Mach number range, and various flow conditions along the chord of the model. For the transitional boundary layer, Fig.5(a), there is a slight suggestion of non-linearity. The paucity and poor quality of the data in Fig.6(a), arise from their having been obtained from the first run (see section 4).

Stanton numbers were estimated by an intermediate temperature method, for the following conditions:-

(a) <u>Ahead of the corner</u>

(i) The laminar boundary layer on an ideal flat plate with a thin, sharp leading edge.

(ii) The flat plate turbulent boundary layer, with effective origin at the leading edge.

(b) Aft of the corner

The flat plate turbulent boundary layer appropriate to the Mach number and unit Reynolds number downstream of the single, oblique shock wave; the momentum thickness immediately behind the shock was calculated from the momentum thickness of (a)(ii) above at the corner, allowance being made for the pressure jump at the shock wave.

Since the surface temperatures in the tests were never far from recovery temperature, estimates were made only for recovery surface temperatures. The formulae used in the estimates were those recommended in Ref.7. The specific heat of air was assumed constant. For both laminar and turbulent flow, the intermediate temperature (T^x) was taken as:-

$$T^x = T_e + 0.5(T_w - T_e) + 0.22(T_r - T_e) \quad ,$$

where T_e = air static temperature just outside the boundary layer.

For $T_w = T_r$,

$$T^x = T_e + 0.72(T_r - T_e) \quad ;$$

i.e.

$$\frac{T^x}{T_e} = 1 + 0.72\, r\, \frac{(\gamma - 1)}{2} M_e^2 \quad ,$$

with M_e = Mach number just outside the boundary layer.

The recovery factor, r, is given by:-

$$r = \left(P_r^x\right)^{\frac{1}{2}} \quad ,$$

for laminar layers, P_r^* being the Prandtl number at temperature T^x; and

$$r = 0.89$$

for turbulent layers.

Reynolds analogy factors between Stanton numbers (S_T) and skin friction coefficients (c_f) were assumed, giving final formulae, for an isothermal wall:-

$$S_T = 0.332 \left(P_r^x\right)^{-2/3} \left(R_x\right)^{-\frac{1}{2}} \left(\frac{T_e}{T^x} \frac{\mu^x}{\mu_e}\right)^{\frac{1}{2}} \text{ for laminar flow} \quad ,$$

and

$$S_T = 0.288 \times 0.61 \left(\frac{T_e}{T^x}\right)\left[\log_{10} \left(R_x \frac{T_e}{T^x} \frac{\mu_e}{\mu^x}\right)\right]^{-2.45} \text{ for turbulent flow} \quad .$$

In these formulae, R_x is the Reynolds number formed from fluid properties just outside the boundary layer and the distance x from the origin of the layer. The coefficient of viscosity of air is, as usual, denoted by μ.

The ratios of the momentum thicknesses (δ_2) on either side of the corner shock wave were obtained from Nash's[8] formula:-

$$(\rho_e \ u_e \ M_e^2 \ \delta_2)_2 = (\rho_e \ u_e \ M_e^2 \ \delta_2)_1 \quad ,$$

where $(\quad)_1$ and $(\quad)_2$ denote conditions upstream and downstream of the shock wave.

Of several available formulae quoted by Cooke[9], this is the simplest.

6 RESULTS

6.1 Pressure

Pressures were scaled by taking the average pressure well ahead of the corner as unity. Since this study concerns heat transfer rather than pressure distributions, Mach numbers, densities, and velocities were taken from measured pressures rather than nominal flow conditions. Flow changes across the corner correspond to a corner angle of $15.1^\circ \pm 0.1^\circ$, which agrees satisfactorily with the geometrical angle.

The pressure distributions, which confirm the absence of any significant separation at the test Reynolds numbers, are illustrated in Fig.7.

6.2 Heat flow at $M_1 = 4.36$

Since the results of all test are qualitatively similar, detailed description will be confined to one test, namely that illustrated in Fig.8, for which $M_1 = 4.36$.

6.2.1 Region ahead of corner compression

The recovery factors shown in Fig.8(b) rise to a peak before falling away towards the turbulent boundary layer value of 0.89. This behaviour, which is a characteristic of transition regions between laminar and turbulent flow[10], is broadly consistent with the Stanton numbers of Fig.8(c). In the same region, Stanton numbers rise from values appropriate to a laminar layer, finally reaching some 75% of the estimated values for a turbulent layer. Comparison of recovery factors and Stanton number suggests that transition affects the former earlier than the latter, and recovery factors continue to be slightly affected after Stanton numbers have apparently reached their final level.

6.2.2 Region near corner

Recovery factors, whether derived using upstream Mach number (M_1) and corresponding static temperature (T_1) or conditions at the lower Mach numbers associated with the corner compression, fall appreciably reaching a minimum slightly downstream of the corner. Stanton numbers on the other hand, rise sharply if defined using density and velocity ahead of the compression, but remain constant if estimated local density and velocity are used. Local density and velocity were estimated by assuming that $\frac{(\rho u)_{local}}{\rho_1 u_1}$ was the same function of $\frac{(p)_{local}}{p_1}$ as it would be if the pressure rise from p_1 to $(p)_{local}$ were produced by a single oblique shock. Thus $(\rho u)_{local}$ were found by using tables of flow changes through oblique shocks in conjunction with the pressure distributions of Fig.7. As may be seen from the lower line in Fig.8(a), wall temperature rose appreciably through the compression region when heat was being transferred to the model.

6.2.3 Region downstream of corner compression

Both recovery factor and Stanton number rise initially, the former tending to return to the normal level for a turbulent boundary layer. Stanton numbers based on local density and velocity tend on average to some 80% of the estimated values behind the corner shock wave. Apparently, the proportionate increase of Stanton number through the shock agrees fairly well with the theoretical estimate except in the immediate neighbourhood of the corner. On both sides of the compression region, however, the Stanton number levels from experiment are below the estimates.

In the forward part of the region especially, the true dimensional rate of heat transfer is much lower than would be estimated for the measured surface temperature because of the combined effect of low Stanton number and low recovery factor.

6.3 Effects of reducing Mach number ahead of corner

Test results for M_1 ranging from 3.97 to 2.495 are shown in Figs.9 to 12. Reduction of Mach number ahead of the corner tends to move transition nearer to the leading edge of the model. Reynolds number at the end of transition, as indicated by recovery factors, falls slightly from about 4.5×10^6 at $M_1 = 4.36$ to 3.9×10^6 at $M_1 = 3.59$. At the remaining Mach numbers, $M_1 = 3.23$, 2.495, transition appears to be ahead of the first instrumented station. This implies that transition is complete at Reynolds numbers below 3.3×10^6.

Ahead of the corner Stanton numbers fall further below the estimates as M_1 is reduced, until at $M_1 = 2.495$ they are only about 50% of expected values.

Downstream of the corner, the principal effect of Mach number reduction is to delay the return of recovery factor to the flat-plate boundary layer level. For $M_1 \leqslant 3.59$ this return does not occur within the length of the model. The probable reason for this low-Mach number behaviour is that the 15° corner angle is then close to the limiting angle for attached flow. According to Kuehn[11], this limiting angle falls from about 23° when $M_1 = 4$ to 17° when $M_1 = 2.5$ at relevant Reynolds numbers.

6.4 Effect of unsteadiness in surface temperature on heat flow

During the $M_1 = 3.97$ run, data were recorded at frequent intervals during a period when coolant temperature was allowed to vary. Time histories of heat flow and model surface temperature are shown in Fig.13. In Fig.14 these measurements are compared with the mean relation between heat flow and temperature for nominally steady conditions. Analysis of the deviations of heat flows from the steady-state relation shows that, at given temperature, the error in a heat flow measurement correlates well with the mean rate of change of temperature during some 5 or 6 minutes preceding the acquisition of the data; that is in Fig.13, a slope A-A rather than B-B, determines the error of the data at time C. A mean change of $\frac{1}{4}{}^\circ$C per minute in model surface temperature, preceding time C produces an error of about 2×10^{-5} in non-dimensional heat flow measured at that time. This numerical result is not general: it would be expected to depend on the thermal properties of the thermocouple, skin and heatmeter to which the measurements relate.

7 GENERAL DISCUSSION

The most striking result of these tests is that on both sides of the corner, heat transfer through the turbulent boundary layers appears to be much lower than one would expect. This and the considerable scatter of the Stanton numbers foster suspicion of the accuracy of the heatmeter calibrations. A brief attempt to calibrate some of the meters in the model indicated that, in this environment, these meters may be some 10% less sensitive than in the maker's calibrating apparatus. Even if the Stanton numbers were raised by this amount, they would still lie considerably below the estimates*.

It is thought that errors in the measurement of surface temperature would not be large enough to explain the remaining discrepancy. Such errors would, however, be in the correct sense, because the thermocouples would tend to measure the lower temperature at some point within the skin, if they failed to measure surface temperature. Some indication of the possible size of these errors may be gained from the fact that the temperature gradient in the resin skin is some 40-50°C per inch at a heat flow of 0.1 CHU/ft^2 sec. The progressive divergence between theory and experiment as Mach number falls is consistent with error in the temperature measurements. This is because the difference between recovery and surface temperatures needed to generate a given heat transfer, falls with Mach number; consequently measurement errors become more important at the lower Mach numbers.

The experimental results have been presented as they were obtained: with neither heat flux nor wall temperature constant along the model. Reliable methods for relating Stanton numbers in compressible flow at arbitrary wall conditions to Stanton numbers at standard conditions such as an isothermal wall do not, to the authors' knowledge, exist. Such methods are needed in order that heat transfer rates and wall temperatures for real vehicles may be calculated, since the temperature and heat flow distributions will depend not only on aerodynamic (convective) heat transfer, but also on internal and external radiation, internal heat paths provided by the structure, and the coolers or heat sinks contained therein. The interaction of these factors can correctly be obtained only if heat transfer coefficients appropriate to any arbitrary wall conditions are known.

In incompressible flow, methods have been developed for the effects of variable wall temperature (actual distributions being approximated by combinations of "step" and linear "ramp" changes of temperature[12]), and for the effects of transition[13]. For compressible flow the effect of a step change in wall temperature is examined in Ref.14.

8 CONCLUSIONS

Heat transfer measurements in the vicinity of a 15° compression corner, with approach Mach numbers ranging from 2.495 to 4.36 have shown the following features:-

---

* See footnote to p. 14.

(1) Measured Stanton numbers for turbulent flow are lower than had been estimated; the accuracy of these measurements is, however, uncertain*.

(2) Away from the immediate vicinity of the corner, ratios of Stanton numbers upstream and downstream of the compression are as expected.

(3) Low recovery factors in the immediate neighbourhood of the compression lead to low heat transfer; this region extends furthest at the lowest approach Mach numbers where the corner shock wave is nearly strong enough to separate the boundary layer. The measured recovery factors are probably reliable, since heat conduction from temperature and heat sensors, a likely source of error in the tests as a whole, should become unimportant as recovery temperature is approached.

---

* After this Report was first issued, further calibrations of single heatmeters were performed by staff of the 8 ft Supersonic Tunnel at R.A.E. Bedford. The new calibrations indicate that the calibrating technique evolved by Hatfield[2] and used by heatmeter manufacturers overestimates heatmeter sensitivity by one-third. Complete acceptance of the new calibrations, which should be more accurate than those mentioned on page 13, would bring the Stanton numbers of this experiment much closer to estimated values.

Table 1

Positions of instrumented stations

(Distances from leading edge are along the airswept surface.)

Distance from leading edge (inches)	Static pressure tap (offset: port or starboard) (inches)	Heatmeter and thermocouple (offset: port or starboard) (inches)
2.9	0.6 S	0.4 P
4.0	0.6 P	0.4 S
5.1	0.6 S	0.4 P
5.35	-	0.4 S
5.6	0.6 S	0.4 P
5.85	0.6 P	0.4 S
6.1	-	0.4 P
6.35	0.6 P	0.4 S
6.6	0.6 S	-
6.85	0.6 P	0.4 S
7.1	0.6 S	0.4 P
(7.25)	(Corner)	
7.4	0.6 P	0.4 S
7.65	0.6 S	0.4 P
7.9	0.6 P	0.4 S
8.15	0.6 S	0.4 P
9.25	-	0.4 S
10.35	0.6 S	0.4 P

Note:- Spaces in the table denote stations where instruments were unserviceable; additionally, at 8.15 inches from leading edge, no heat flow data were obtained in the test at $M_1 = 4.36$.

Table 2

Summary of test conditions

Nominal total pressure of free stream 220 inHg
Nominal total temperature of free stream 40°C

Ahead of corner		Aft of corner		Max. free stream total pressure for visible separation
Mach number	"Unit" Reynolds number	Mach number	"Unit" Reynolds number	
-	1/ft	-	1/ft	inHg
2.495	13.25×10^6	1.87	16.33×10^6	45
3.23	13.21×10^6	2.41	17.70×10^6	45
3.59	11.83×10^6	2.65	15.73×10^6	47
3.97	9.92×10^6	2.91	13.18×10^6	70
4.36	8.33×10^6	3.20	11.58×10^6	100

SYMBOLS

C_p	specific heat of air at constant pressure
M	Mach number
Q	heat transfer rate per unit area
R_x	Reynolds number $= \dfrac{\rho_e u_e x}{\mu_e}$
r	recovery factor
S_T	Stanton number $= Q/\rho u C_p(T_r - T_w)$
T	temperature
T_o	total temperature in main stream
u	air velocity
x	distance from virtual origin of boundary layer
γ	ratio of specific heats for air
δ_2	momentum thickness of boundary layer
μ	coefficient of viscosity for air
π	non-dimensional heat flow rate
ρ	air density
τ	non-dimensional surface temperature

Superscript

x	intermediate temperature

Suffixes

a	reference condition
e	outer edge of boundary layer
r	zero convective heat transfer
w	model surface
1	ahead of corner compression
2	downstream of corner compression

REFERENCES

No.	Author	Title, etc
1	A. Naysmith	Heat transfer and boundary layer measurements in a region of supersonic flow separation and reattachment. R.A.E. Tech. Note Aero 2558, (A.R.C. 20601) May 1958
2	H.S. Hatfield F.J. Wilkins	A new heat flow meter. J. of Scientific Instruments, Vol.27, Jan. 1950
3	J. Poole	A description of the R.A.E. high supersonic speed tunnel. R.A.E. Tech. Note Aero 2678, 1960
4	D.R. Andrews	Some notes on the model testing facilities afforded by the high supersonic speed wind tunnel at R.A.E. Bedford. R.A.E. Tech. Note Aero 2582, (A.R.C. 20922) August 1958
5	A.C. Browning J.F.W. Crane R.J. Monaghan	Measurements of the effect of surface cooling on boundary layer transition on a 15° cone. Part I. Tests at M = 2 and 3 in an 8 inch × 9 inch wind tunnel at R.A.E. Bedford. A.R.C. 19836, C.P. 381, Sept. 1957
6	G.F. Midwood R.W. Hayward	An automatic self-balancing capsule manometer. A.R.C. C.P. 231, July 1955
7	L.F. Crabtree R.L. Dommett J.G. Woodley	Estimation of heat transfer to flat plates, cones and blunt bodies. R.A.E. Tech. Report No.65137 (A.R.C. 27233), July 1965
8	J.F. Nash	An analysis of two-dimensional turbulent base flow, including the effect of the approaching boundary layer. A.R.C. R.and M. 3344, July 1962
9	J.C. Cooke	Separated supersonic flow. R.A.E. Tech. Note Aero 2879 (A.R.C. 24935), March 1963
10	J.L. Potter J.D. Whitfield	Effects of unit Reynolds number, nose bluntness, and roughness on boundary layer transition. AGARD Report No.256, April 1960
11	M. Kuehn	Experimental investigation of the pressure rise required for the incipient separation of turbulent boundary layers in two-dimensional supersonic flow. NASA Memo 1-21-59A, February 1959

)

REFERENCES (CONTD)

No.	Author	Title, etc
12	W.C. Reynolds W.M. Kays S.J. Kline	Heat transfer in the turbulent incompressible boundary layer. III - Arbitrary wall temperature and heat flux. NASA Memo 12-3-58W, December 1958
13	W.C. Reynolds W.M. Kays S.J. Kline	Heat transfer in the turbulent incompressible boundary layer. IV - Effect of location of transition and prediction of heat transfer in a known transition region. NASA Memo 12-4-58W, December 1958
14	R.J. Conti	Heat transfer measurements at a Mach number of 2 in the turbulent boundary layer on a flat plate having a step-wise temperature distribution. NASA TN D-159, November 1959

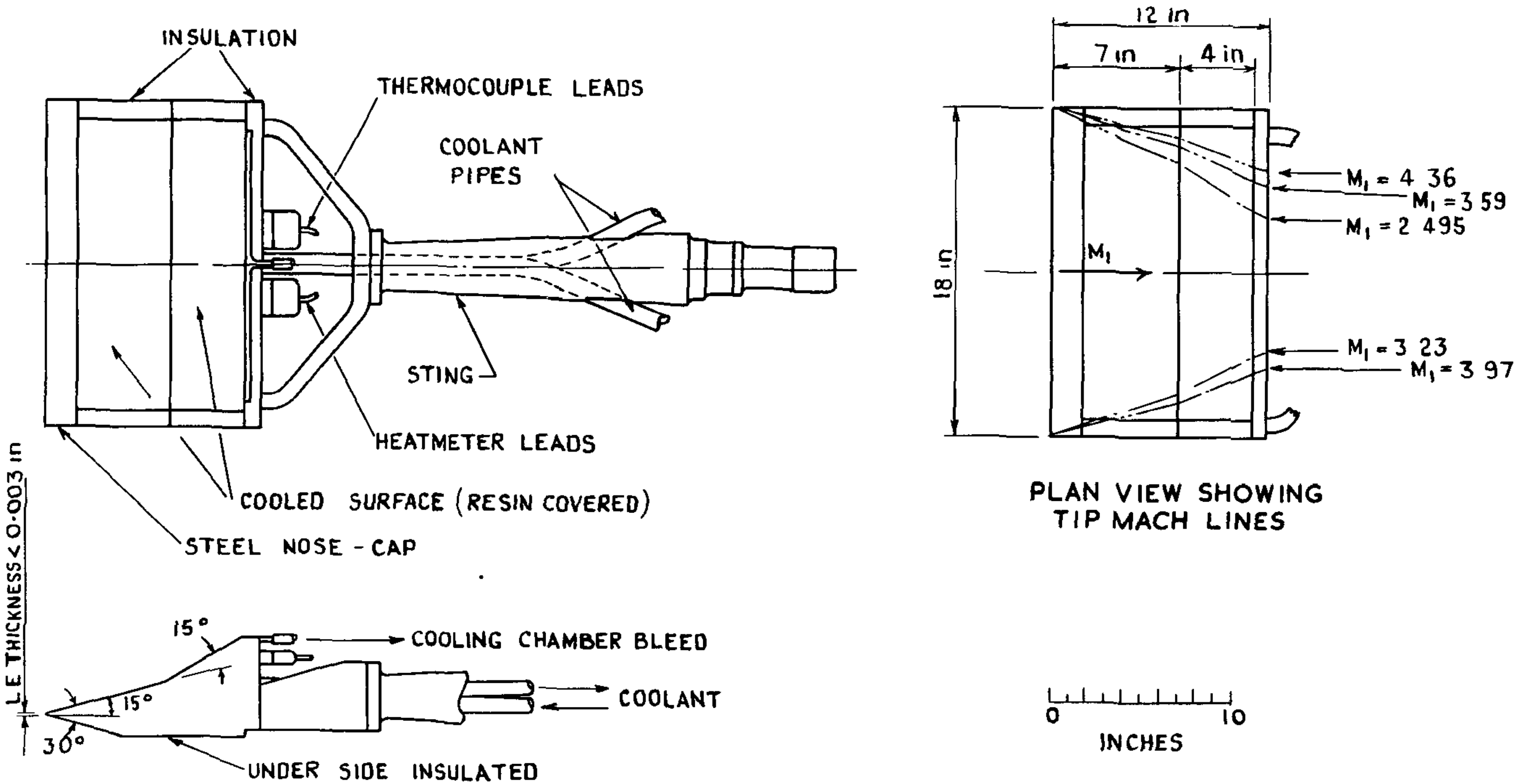

FIG. 1 GENERAL ARRANGEMENT OF MODEL

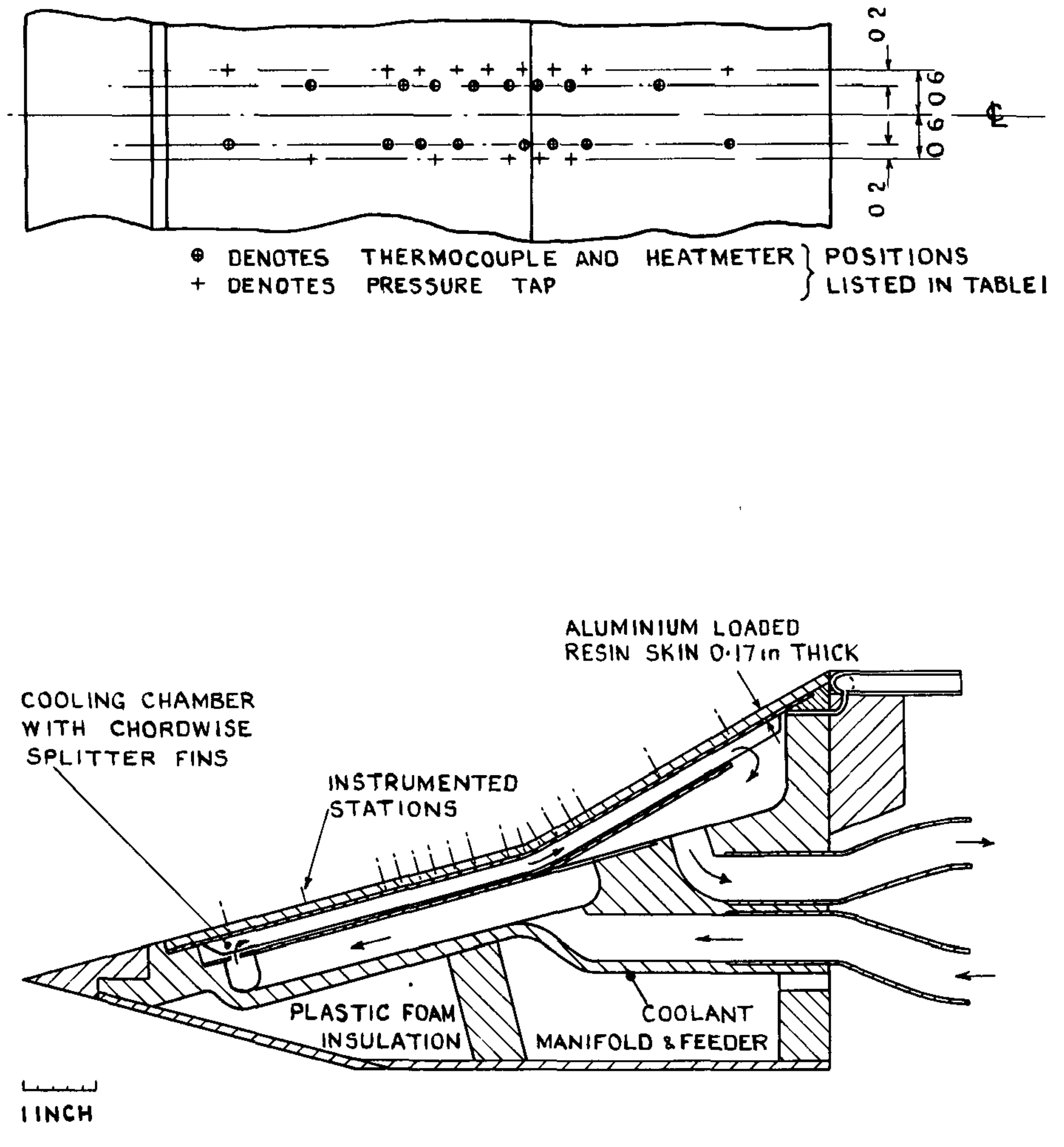

FIG. 2 DETAILS OF MODEL

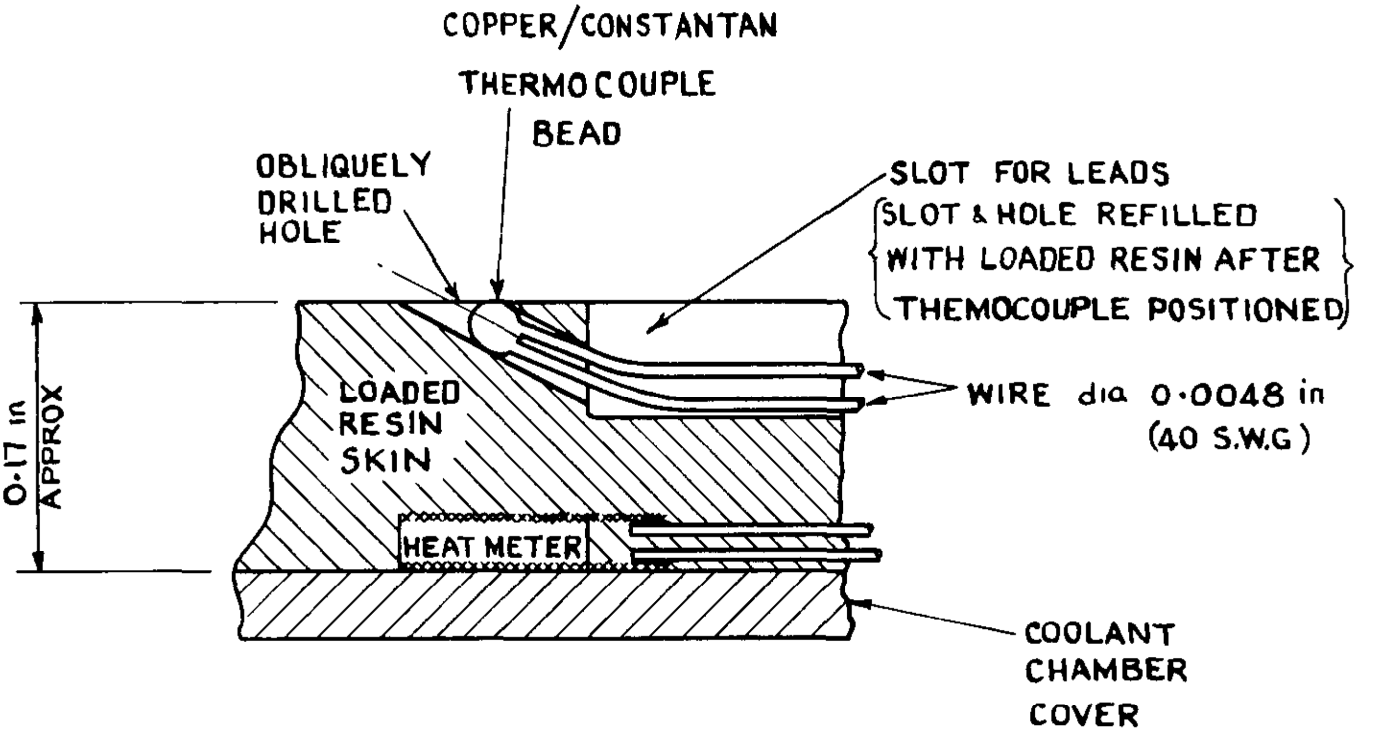

FIG. 3 (a) THERMOCOUPLE & HEATMETER MOUNTING

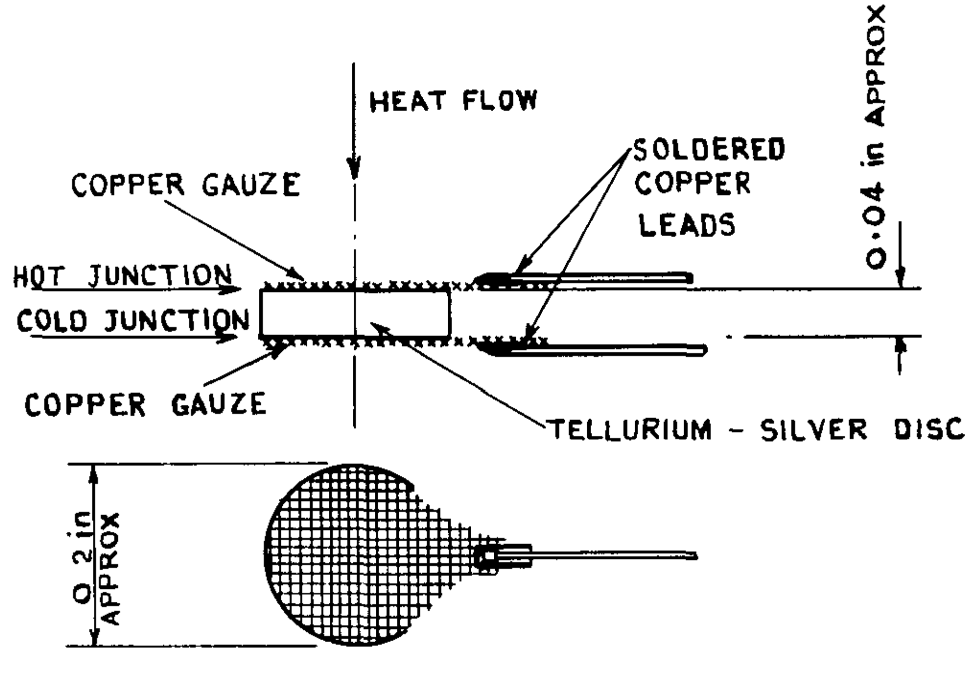

FIG. 3 (b) DIAGRAM OF HEATMETER

FIG. 3 DETAILS OF INSTRUMENTATION

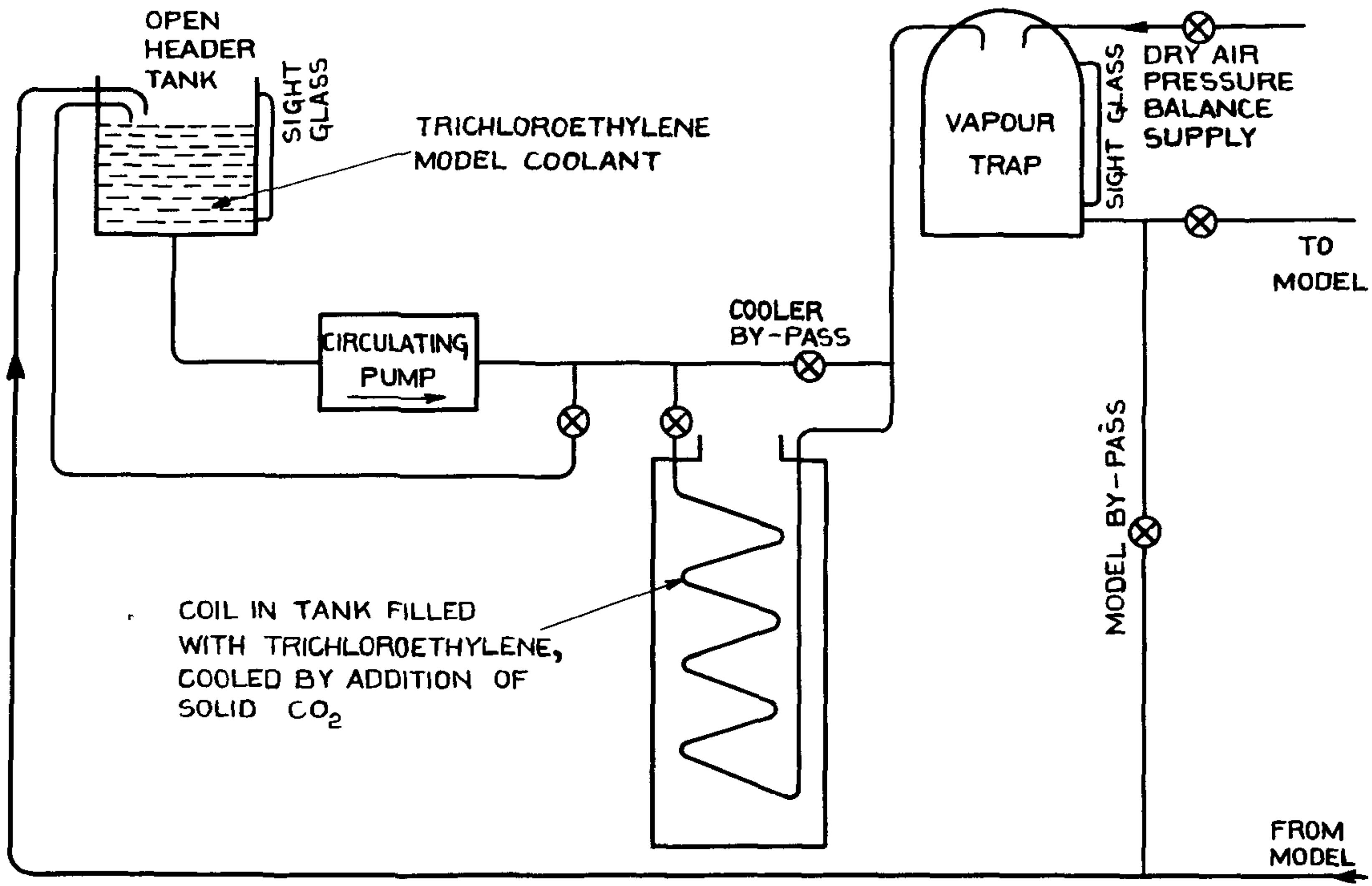

FIG. 4 LINE DIAGRAM OF COOLING RIG

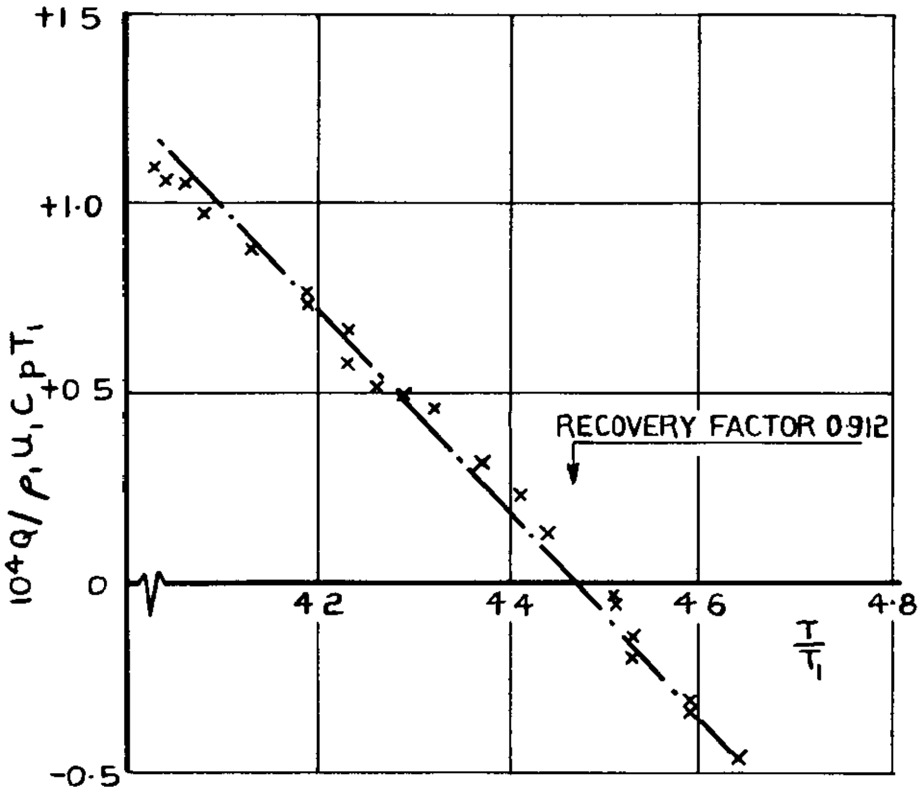

FIG. 5(a) TRANSITIONAL BOUNDARY LAYER; $M_1 = 4.36$
POSITION: 4 in FROM LEADING EDGE

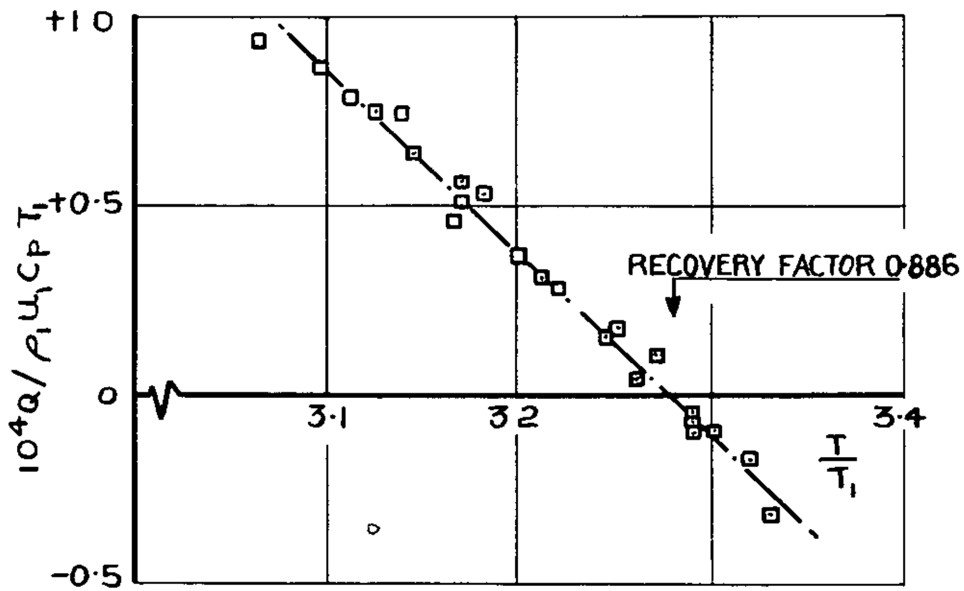

FIG. 5 (b) TURBULENT BOUNDARY LAYER; $M_1 = 3.59$
POSITION : 5.35 in FROM LEADING EDGE

FIG 5 EXAMPLES OF MEASURED RELATIONS BETWEEN HEAT FLOW AND TEMPERATURE UPSTREAM OF CORNER

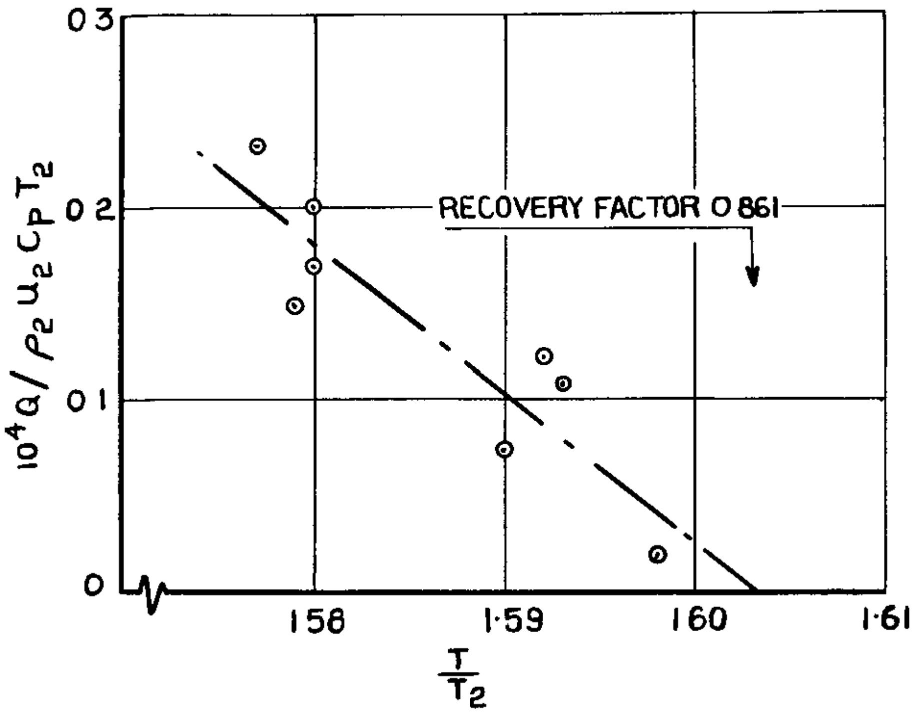

FIG. 6 (a) TURBULENT BOUNDARY LAYER CLOSE TO CORNER COMPRESSION; $M_1 = 2{\cdot}495$, $M_2 = 1{\cdot}87$
POSITION: 9·25 in FROM LEADING EDGE

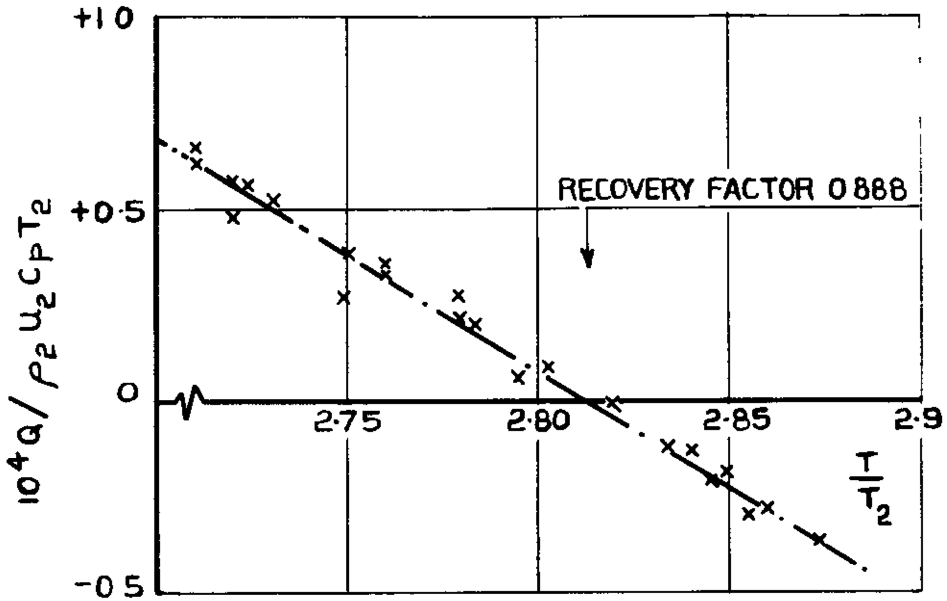

FIG. 6 (b) TURBULENT BOUNDARY LAYER WELL DOWNSTREAM OF CORNER COMPRESSION
$M_1 = 4{\cdot}36$; $M_2 = 3{\cdot}20$
POSITION : 10·35 in FROM LEADING EDGE

FIG. 6 EXAMPLES OF MEASURED RELATIONS BETWEEN HEAT FLOW AND TEMPERATURE DOWNSTREAM OF CORNER

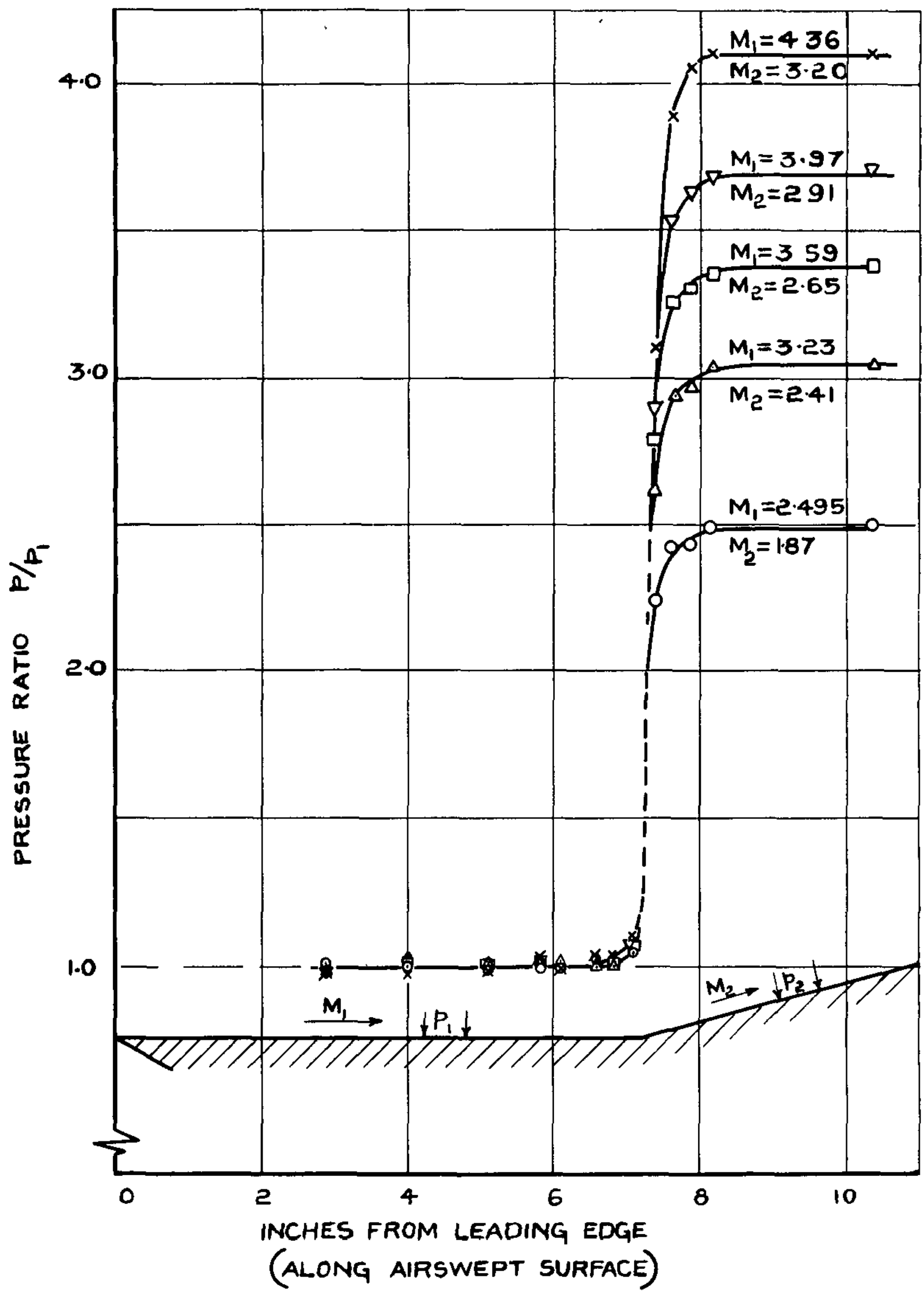

FIG. 7 PRESSURE DISTRIBUTIONS FOR ALL TESTS

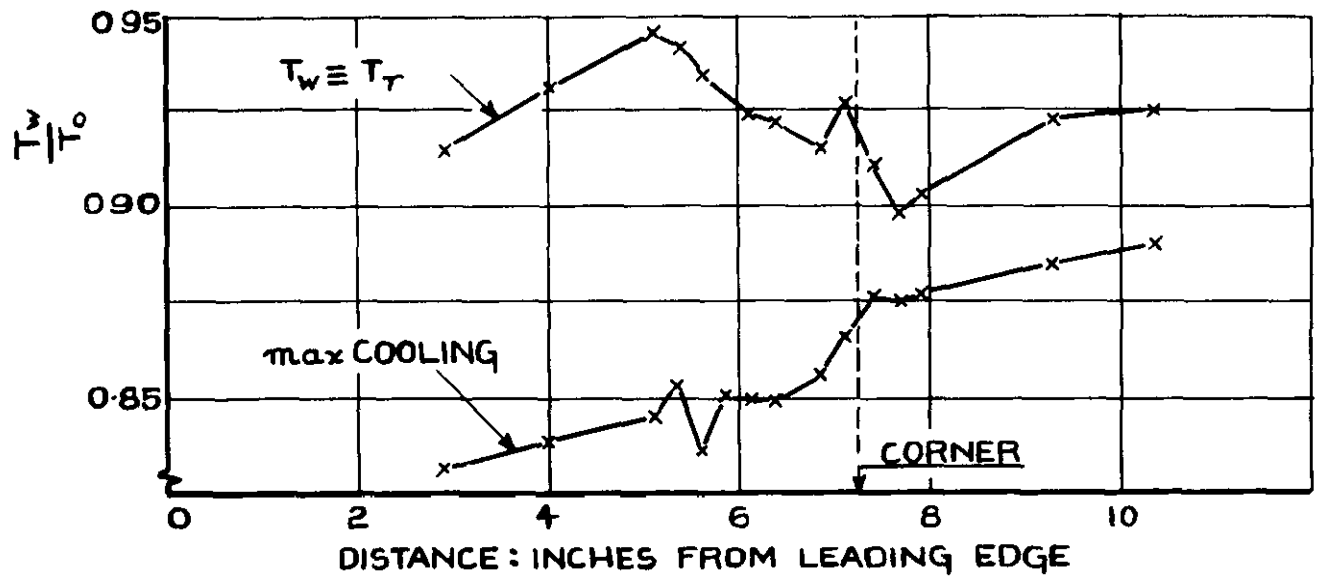

FIG. 8 (a) WALL TEMPERATURES

NATURE OF FLOW	LAMINAR	TRANSITIONAL	TURBULENT	
	NORMAL FLAT PLATE BOUNDARY LAYER		LOCAL EFFECTS OF SHOCK	RETURN TO FLAT PLATE BOUNDARY LAYER

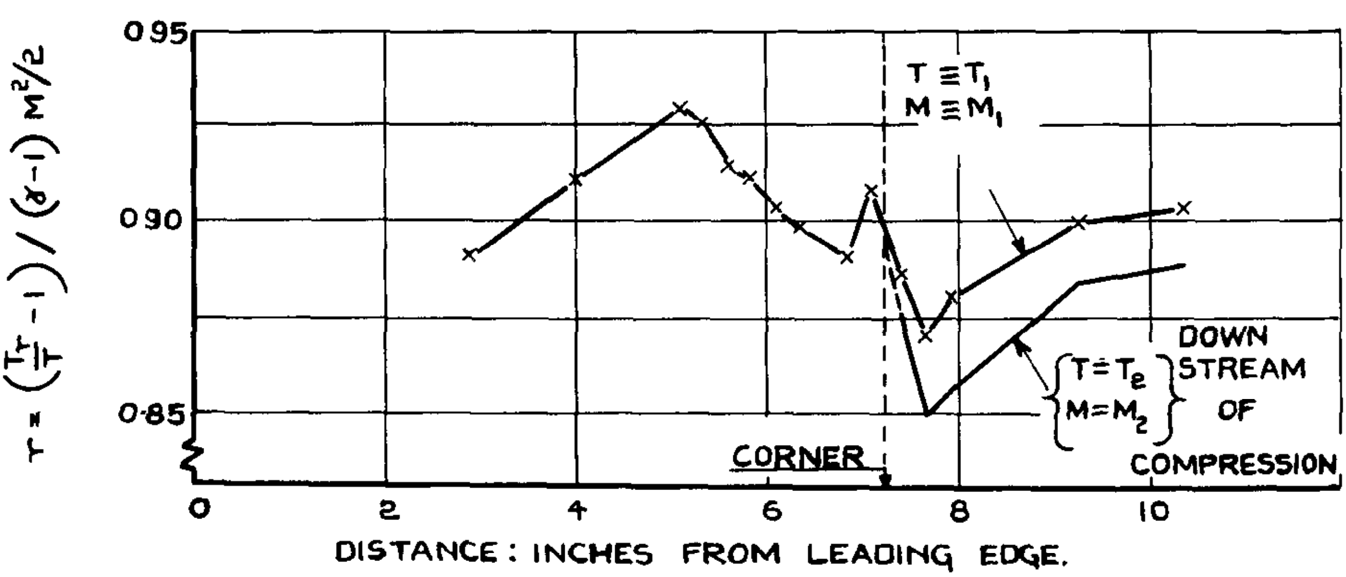

FIG. 8 (b) TEMPERATURE RECOVERY FACTORS

FIG. 8 TEST RESULTS FOR $M_1 = 4{\cdot}36$ (PART I)

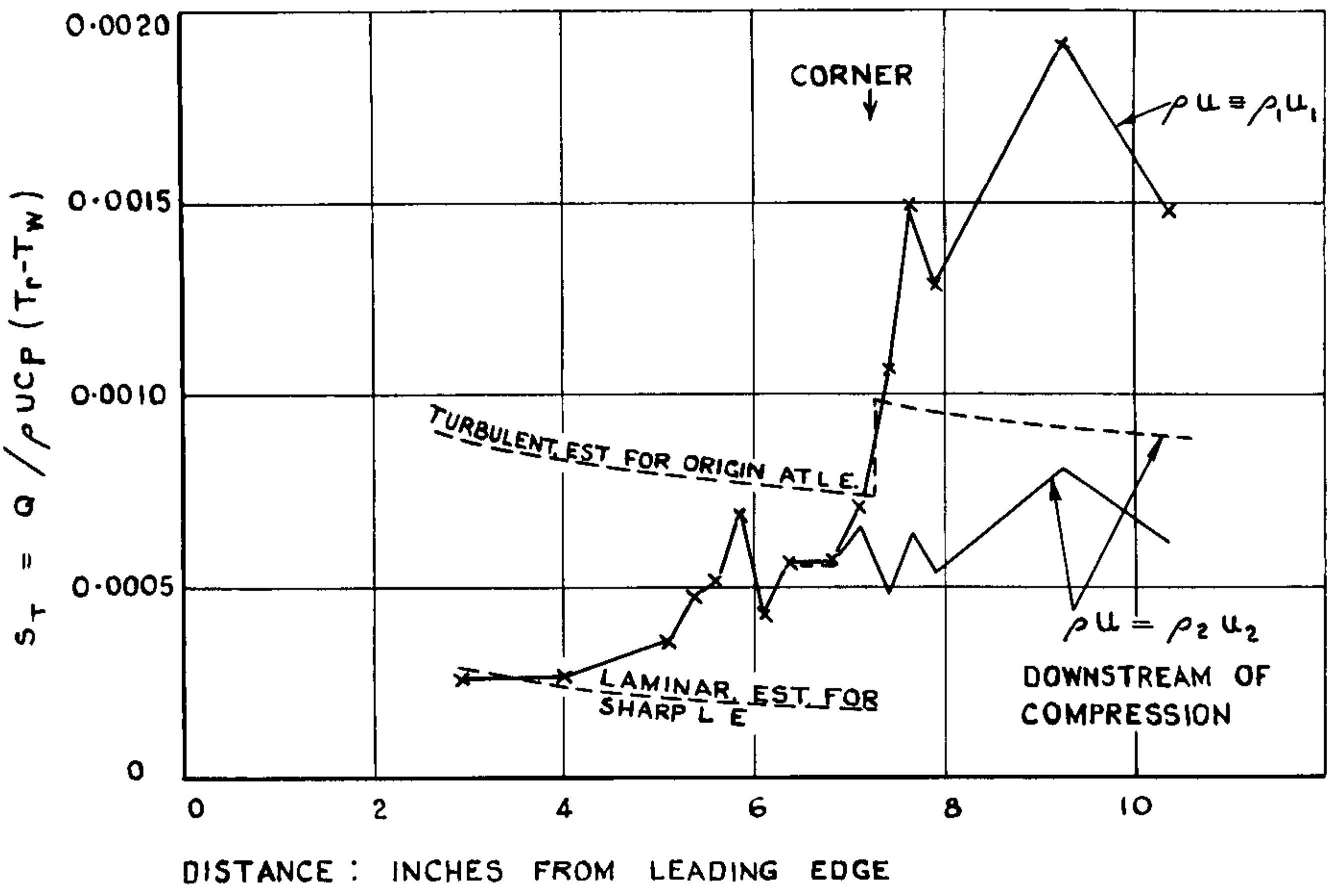

FIG. 8 (c) STANTON NUMBERS

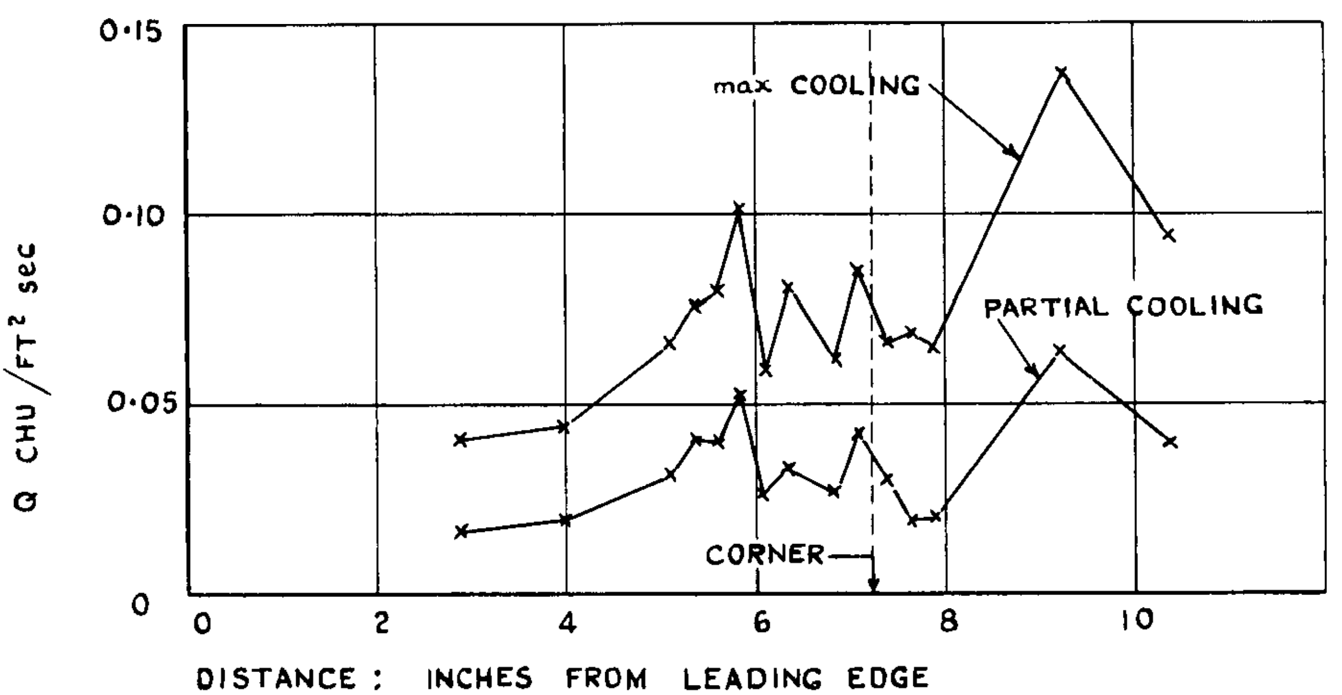

FIG. 8 (d) HEAT TRANSFER RATES

FIG. 8 (CONCLD) TEST RESULTS FOR $M_1 = 4·36$

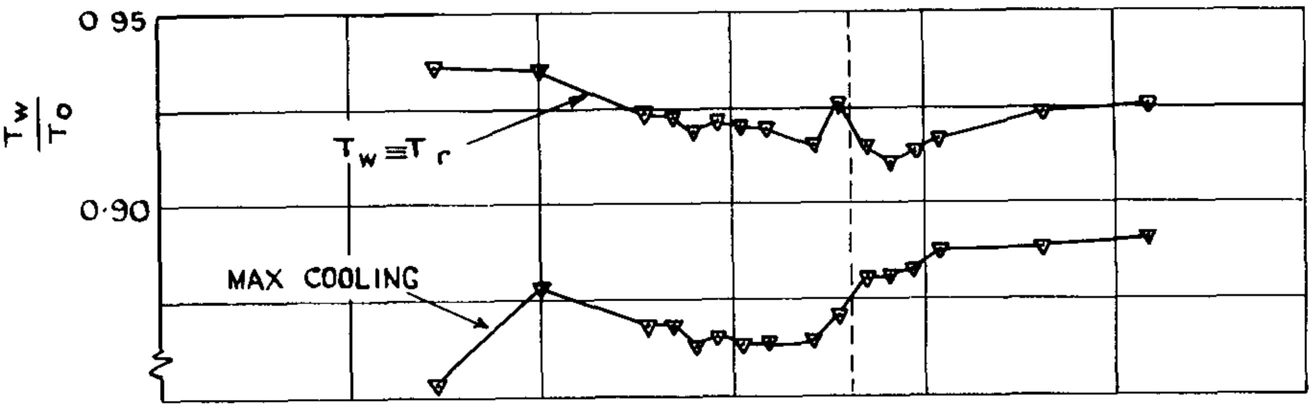

FIG. 9 (a) WALL TEMPERATURES

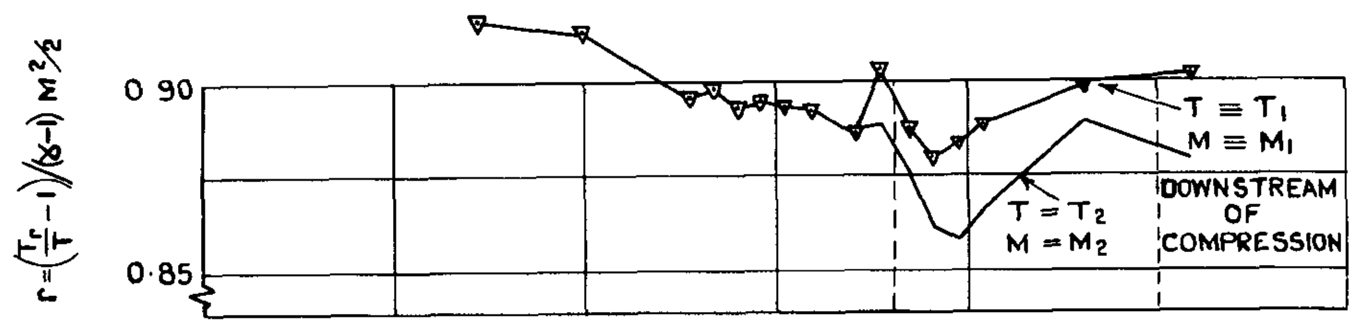

FIG. 9 (b) TEMPERATURE RECOVERY FACTORS

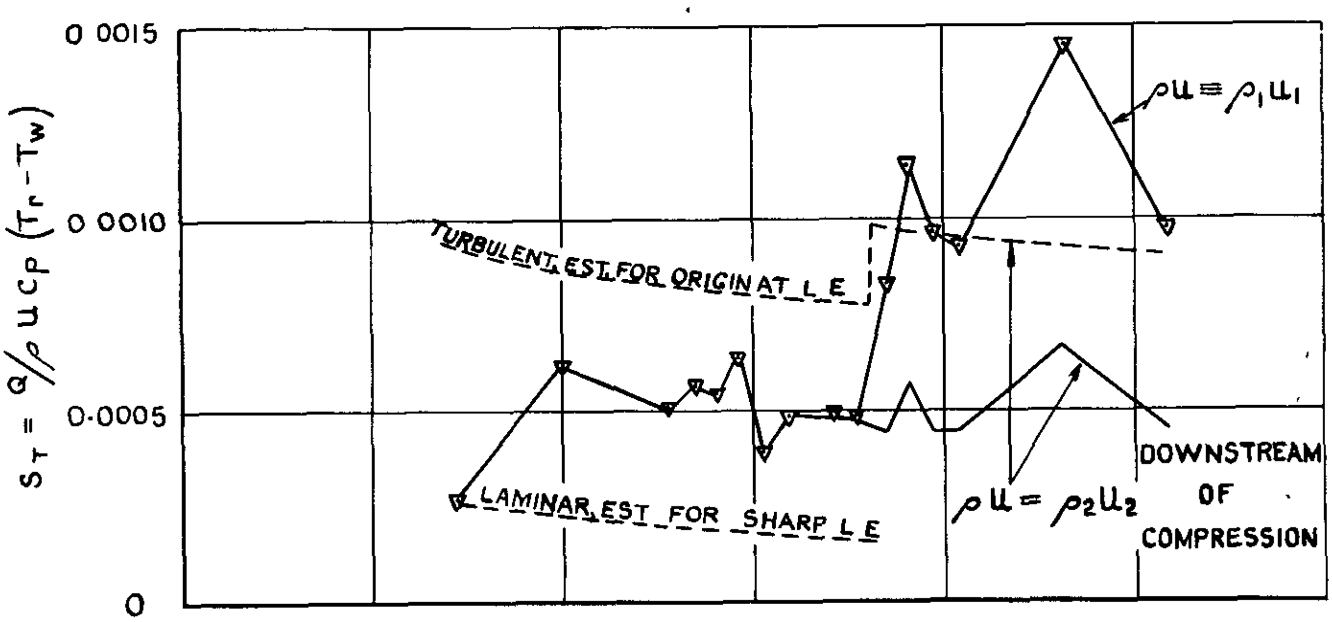

FIG. 9 (c) STANTON NUMBERS

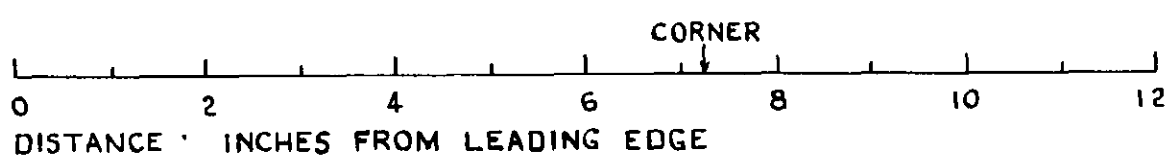

FIG 9 TEST RESULTS FOR $M_1 = 3·97$

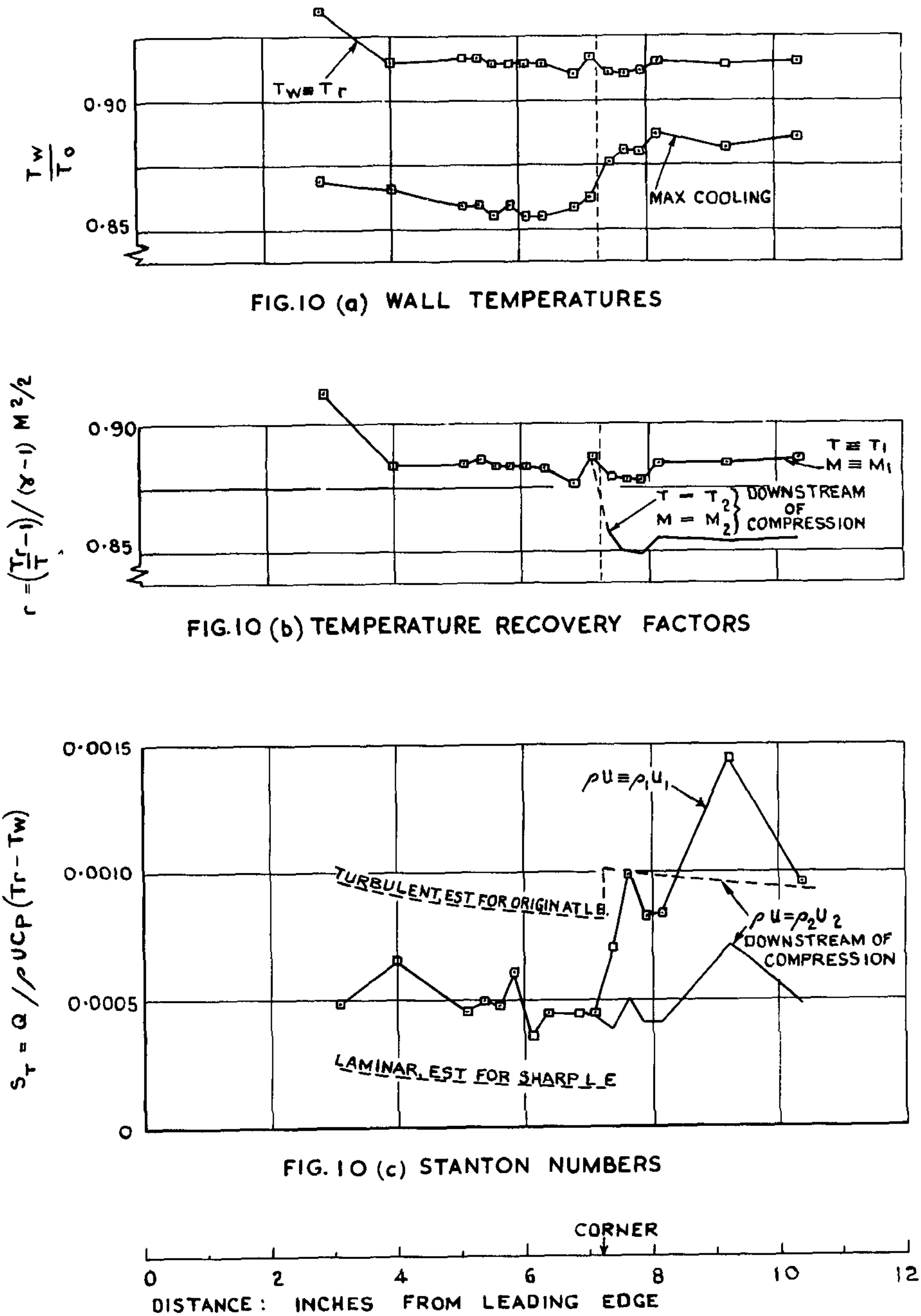

FIG. 10 (a) WALL TEMPERATURES

FIG. 10 (b) TEMPERATURE RECOVERY FACTORS

FIG. 10 (c) STANTON NUMBERS

FIG. 10 TEST RESULTS FOR $M_1 = 3 \cdot 59$

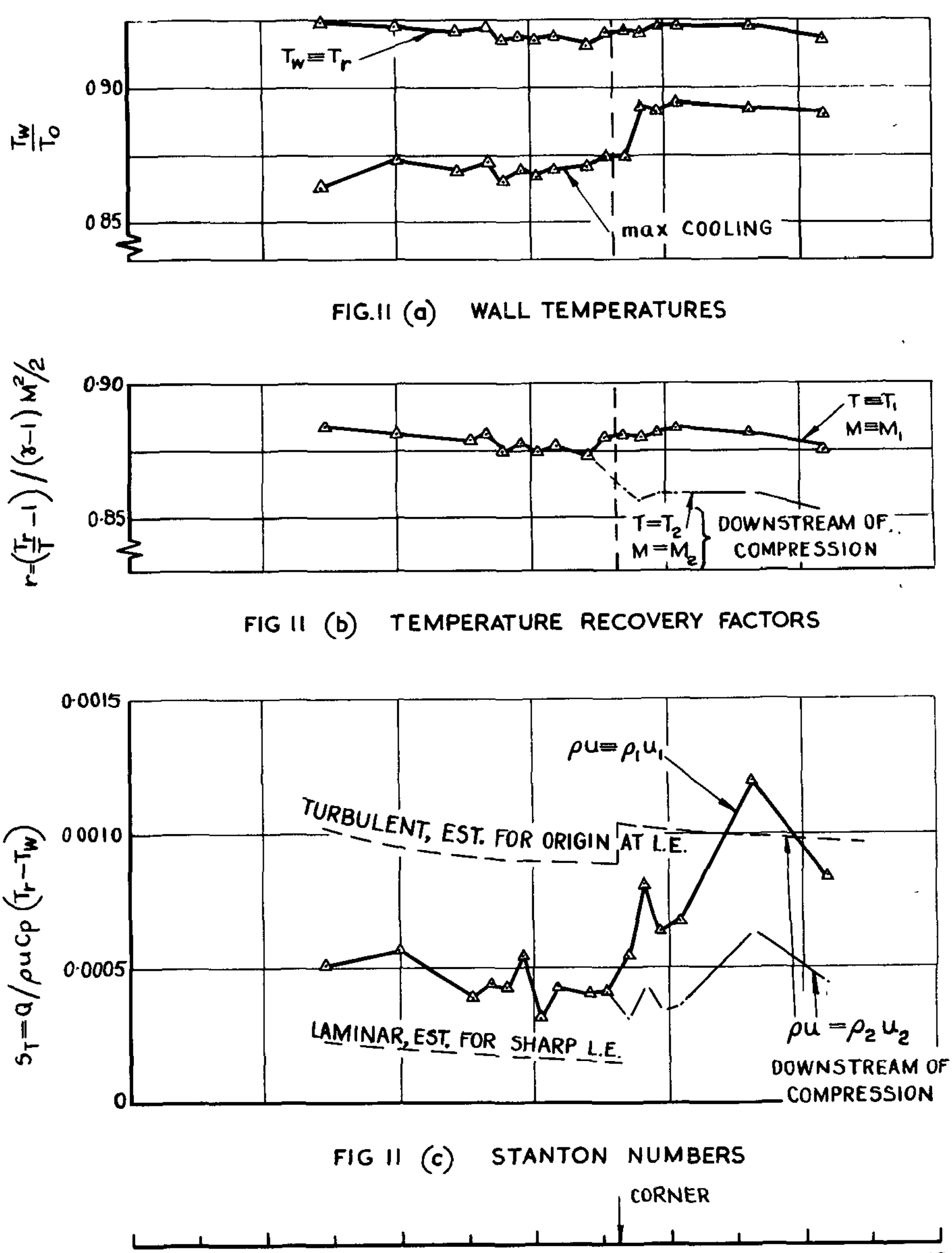

FIG. 11 (a) WALL TEMPERATURES

FIG 11 (b) TEMPERATURE RECOVERY FACTORS

FIG 11 (c) STANTON NUMBERS

FIG. 11 TEST RESULTS FOR $M_1 = 3{\cdot}23$

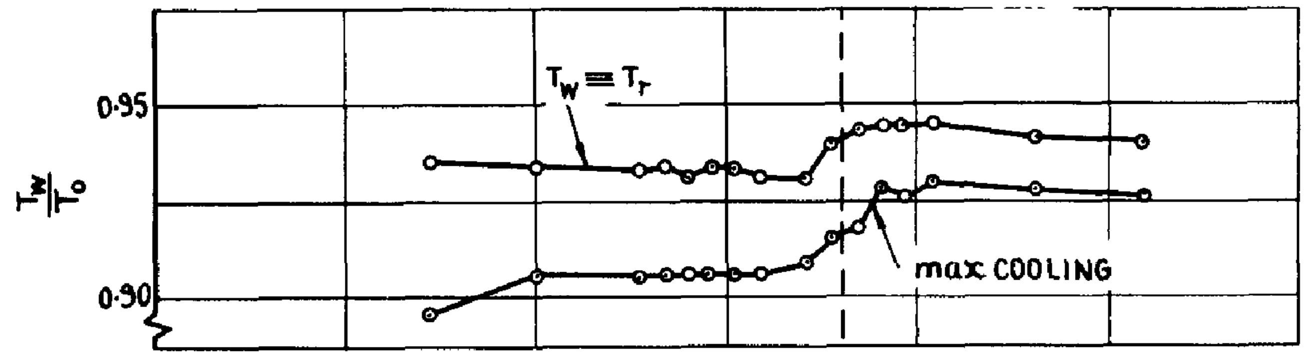

FIG. 12 (a) WALL TEMPERATURES

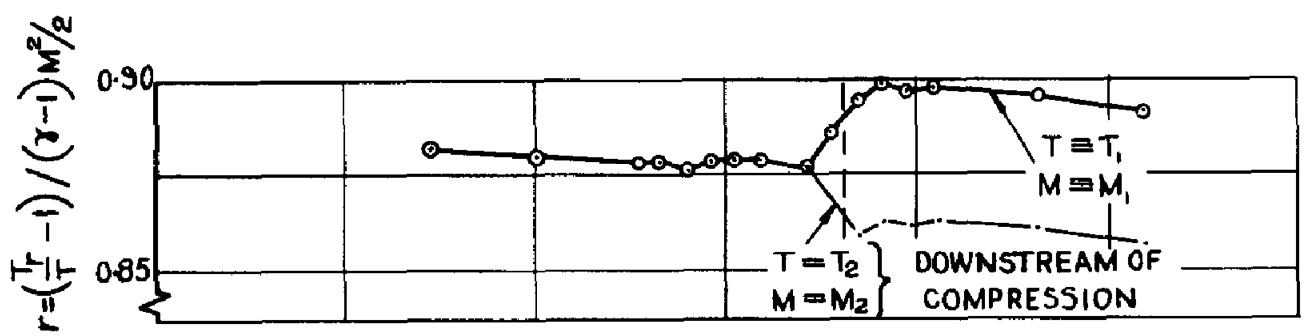

FIG. 12 (b) TEMPERATURE RECOVERY FACTORS

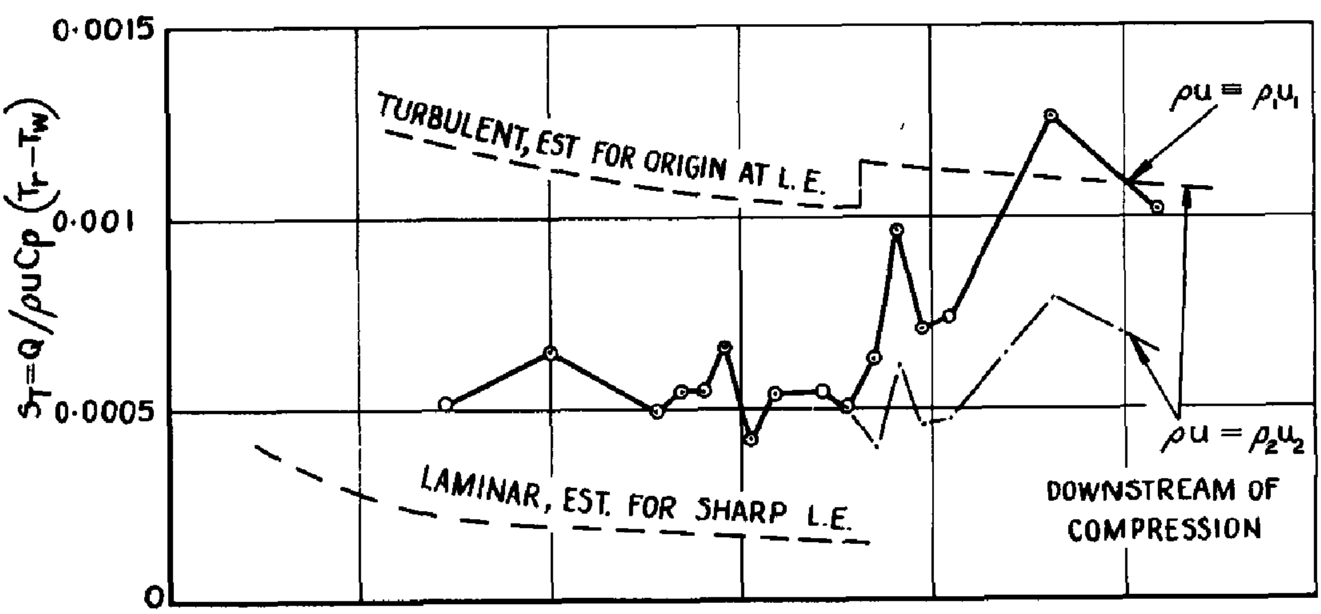

FIG. 12 (c) STANTON NUMBERS

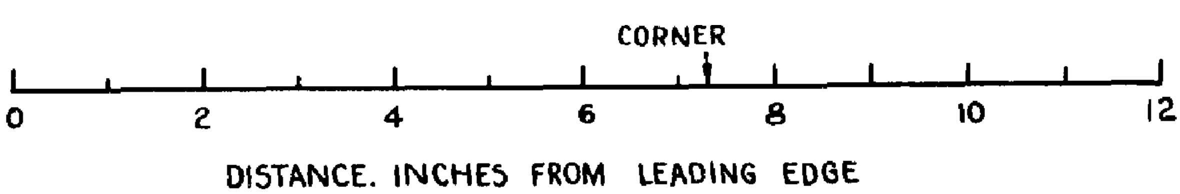

FIG. 12 TEST RESULTS FOR $M_1 = 2{\cdot}495$

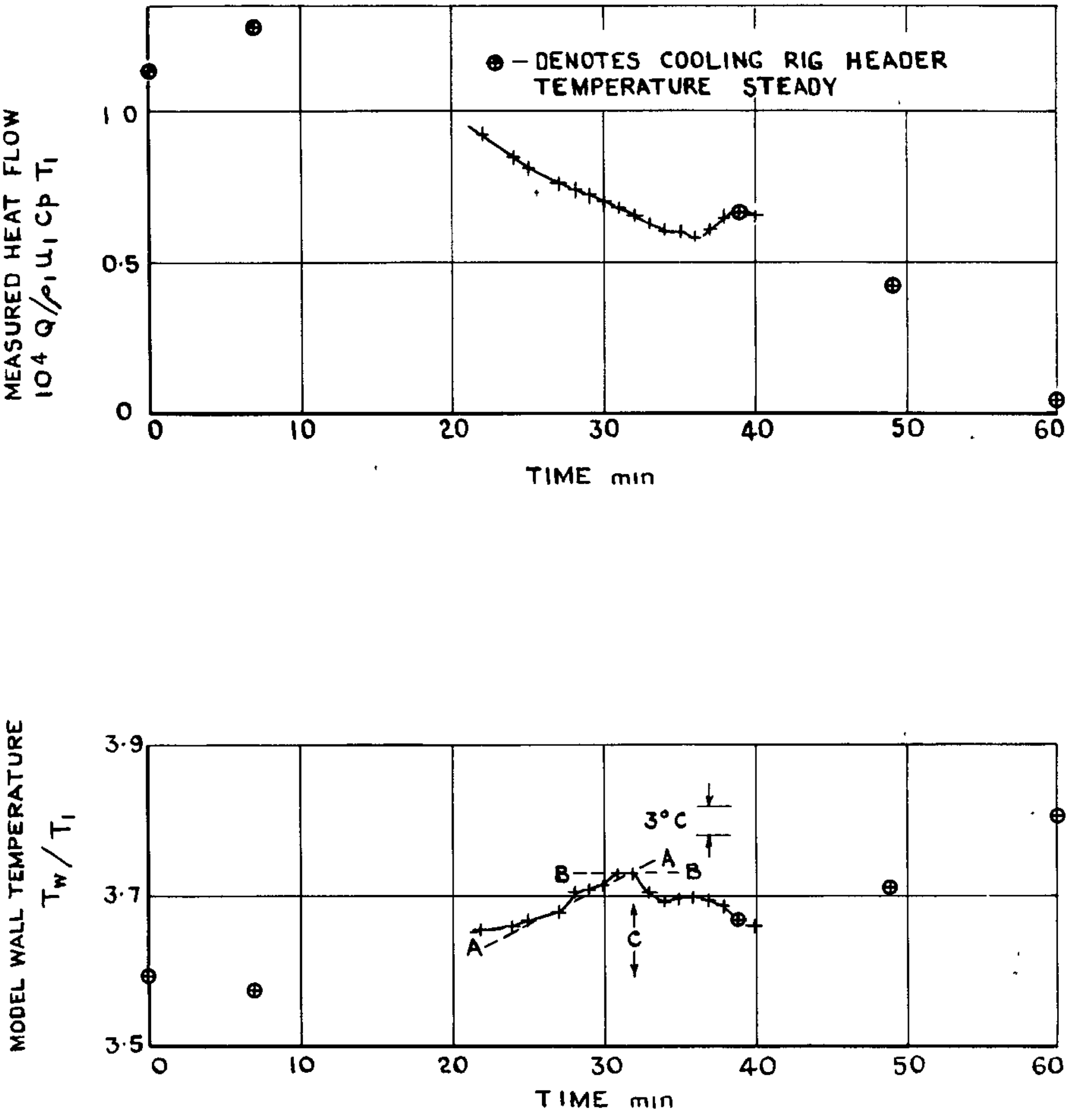

FIG. 13 TIME HISTORIES OF UNSTEADY HEAT FLOW & TEMPERATURE

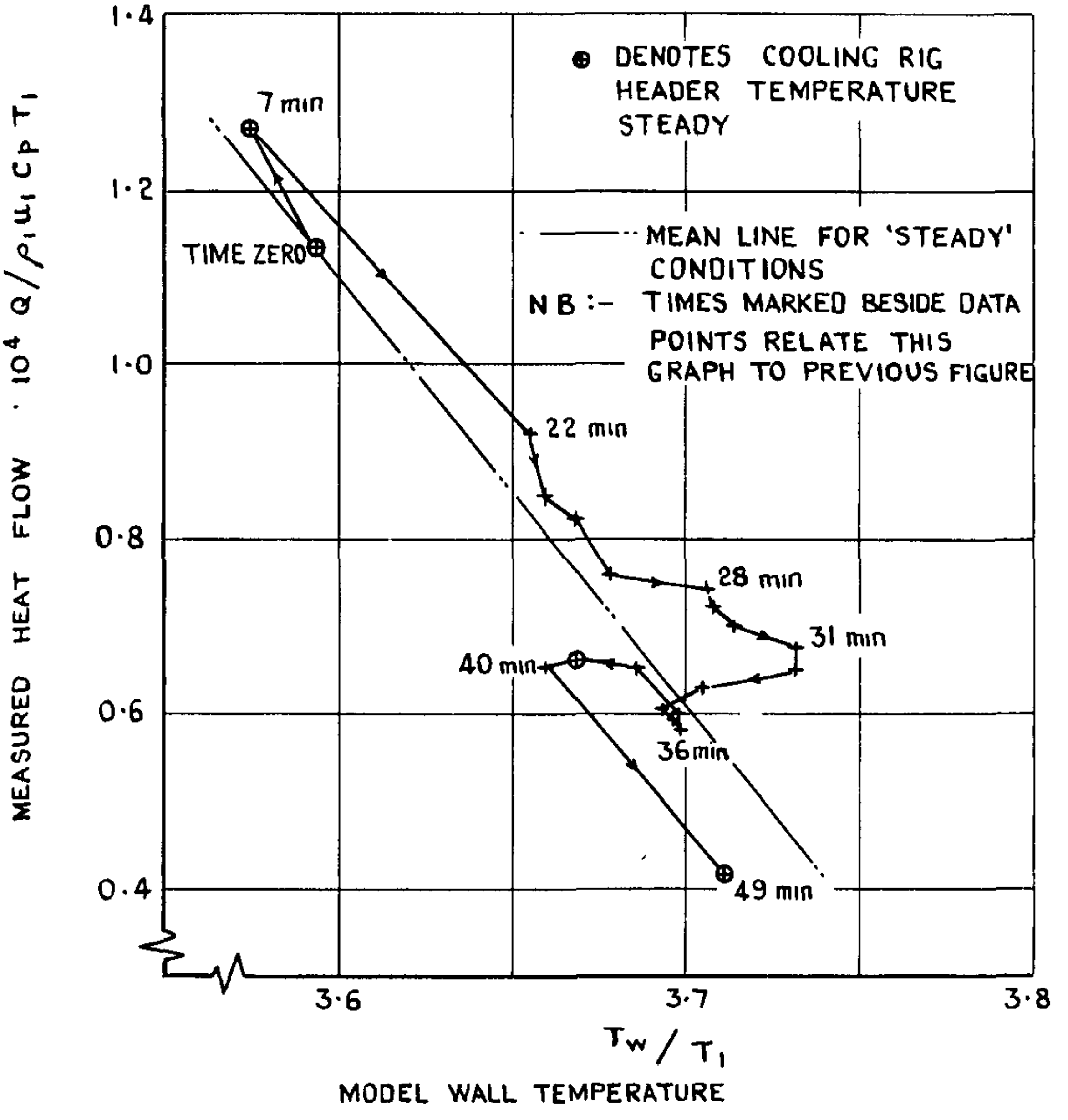

FIG.14 COMPARISON OF 'STEADY' AND 'UNSTEADY' DATA

Printed in England for Her Majesty's Stationery Office by the Royal Aircraft Establishment, Farnborough. Dd.129528. K.4.

A.R.C. C.P. No. 965
June 1966
Hastings, R. C.
Brown, C. S.
Atkinson, Susan

533.6.011.6 :
536.55 :
533.6.011.5 :
532.552

HEAT TRANSFER IN THE VICINITY OF A 15° COMPRESSION CORNER AT MACH NUMBERS FROM 2.5 TO 4.4

Commercially available heatmeters have been used to measure the steady-state heat transfer rates in the vicinity of a compression corner. Results at all Mach numbers are qualitatively similar in that, both ahead and downstream of the corner, the measured heat transfer rate was lower than expected.

In the compression region close to the corner, the adiabatic wall temperatures were also low.

The measuring technique is discussed and some potential sources of error are indicated.

A.R.C. C.P. No. 965
June 1966
Hastings, R. C.
Brown, C. S.
Atkinson, Susan

533.6.011.6 :
536.55 :
533.6.011.5 :
532.552

HEAT TRANSFER IN THE VICINITY OF A 15° COMPRESSION CORNER AT MACH NUMBERS FROM 2.5 TO 4.4

Commercially available heatmeters have been used to measure the steady-state heat transfer rates in the vicinity of a compression corner. Results at all Mach numbers are qualitatively similar in that, both ahead and downstream of the corner, the measured heat transfer rate was lower than expected.

In the compression region close to the corner, the adiabatic wall temperatures were also low.

The measuring technique is discussed and some potential sources of error are indicated.

A.R.C. C.P. No. 965
June 1966
Hastings, R. C.
Brown, C. S.
Akinson, Susan

533.6.011.6 :
536.55 :
533.6.011.5 :
532.552

HEAT TRANSFER IN THE VICINITY OF A 15° COMPRESSION CORNER AT MACH NUMBERS FROM 2.5 TO 4.4

Commercially available heatmeters have been used to measure the steady-state heat transfer rates in the vicinity of a compression corner. Results at all Mach numbers are qualitatively similar in that, both ahead and downstream of the corner, the measured heat transfer rate was lower than expected.

In the compression region close to the corner, the adiabatic wall temperatures were also low.

The measuring Technique is discussed and some potential sources of error are indicated.

DETACHABLE ABSTRACT CARDS

C.P. No. 965

Published by
HER MAJESTY'S STATIONERY OFFICE

To be purchased from
49 High Holborn, London W C 1
423 Oxford Street, London W 1
13A Castle Street, Edinburgh 2
109 St Mary Street, Cardiff
Brazennose Street, Manchester 2
50 Fairfax Street, Bristol 1
35 Smallbrook, Ringway, Birmingham 5
7-11 Linenhall Street, Belfast 2
or through any bookseller

C.P. No. 965

S.O. CODE No. 23-9017-65